

Electrical Supporting Information

A high-power ultrasonic microreactor and its application in gas-liquid mass transfer intensification

Zhengya Dong^{a,b}, Chaoqun Yao^{a,b}, Xiaoli Zhang^c, Jie Xu^c, Guangwen Chen^{a*}, Yuchao Zhao^a,
Quan Yuan^a

^a *Dalian National Laboratory for Clean Energy, Dalian Institute of Chemical Physics, Chinese Academy of Sciences, Dalian 116023, China, gwchen@dicp.ac.cn*

^b *University of Chinese Academy of Sciences, Beijing 100049, China*

^c *Applied Acoustics Institute, Shaanxi Normal University, Xian, Shaanxi 710062, China*

1. One dimension design theory and the calculation of the resonance frequency

The one dimension design theory is often used to design the LUT and calculate the resonance frequency^{1,2}. According to this theory, the half-wave longitudinal resonator can be divided into two quarter-wave resonators by the vibration node plane (Fig. S1(a)). The frequency equations for each of them are

$$\tan k_e l_{c1} = \frac{\rho c_e S}{X_{m1}} \quad (1)$$

$$\tan k_e l_{c2} = \frac{\rho c_e S}{X_{m2}} \quad (2)$$

where l_{c1} and l_{c2} indicate the locations of the node plane in the piezoelectric pieces. X_{m1} and X_{m2} are the impedances of the back and front mass, which depends on their structure, size and property. For the LUT used in our experiment, the impedance of the cylinder back mass is

$$X_{m1} = \rho_1 c_1 S_1 \tan k_1 l_1 \quad (3)$$

The impedance of the circular truncated cone front mass is

$$X_{m2} = \rho_2 c_2 S_2 \frac{Nk_2 l_2 \tan k_2 l_2 + (N-1)^2 \left(\frac{\tan k_2 l_2}{k_2 l_2} - 1 \right)}{Nk_2 l_2 + N(N-1) \tan k_2 l_2} \quad (4)$$

where ρ , k_e , c_e , S and $l_c = l_{c1} + l_{c2}$ are the density, wave number, longitudinal wave speed, cross area and thickness of the piezoelectric pieces; ρ , k_1 , c_1 , l_1 and S_1 are the density, wave number, longitudinal wave speed, length and cross area of the back mass; ρ , k_2 , c_2 , l_2 , S_2 and $N = D_2/D_3$ is the density, wave number, longitudinal wave speed, the back surface area, the front-back surface diameter ratio of the front mass.

The above equations can be used to calculate the resonance frequency of the LUT. They can also be used to design the size of the piezoelectric plates, back and front mass for a LUT with desired frequency. As the ultrasonic microreactor vibrates as a similar longitudinal half-wave resonator, the above equations can also be used to design the ultrasonic microreactor. The size and the structure of the ultrasonic microreactor were shown in Fig. S1(b). The LUT was made of two piezoelectric pieces clamped between a circular truncated cone front mass and a cylinder back mass (stainless steel). As the length of the microreactor plate is close to the diameter of the front surface of the front mass, the two can be regarded as a new circular truncated cone mass with length changing to $47+d$ mm and diameter ratio to $45/74$ (d is the thickness of the microreactor). A MATLAB procedure was used to solve the four equations. The value of the acoustic parameters was displayed in table in table 1. If the thickness of the microreactor pate is too large, the calculated value of l_{c2} will be negative, which means the

vibration node is located at the front mass. For example, when the thickness was chosen to be 5 mm, l_{c2} was calculated to be -0.06 mm . For the convenience of micro-fabrication and tubes connection, the thickness of microreactor should also not be too small. Considering these two points, the thickness was chosen as 3 mm, when the resonance frequency was calculated to be 20.38 kHz and l_{c2} 0.5 mm, which means that the vibration node plane is located at the upper piezoelectric piece.

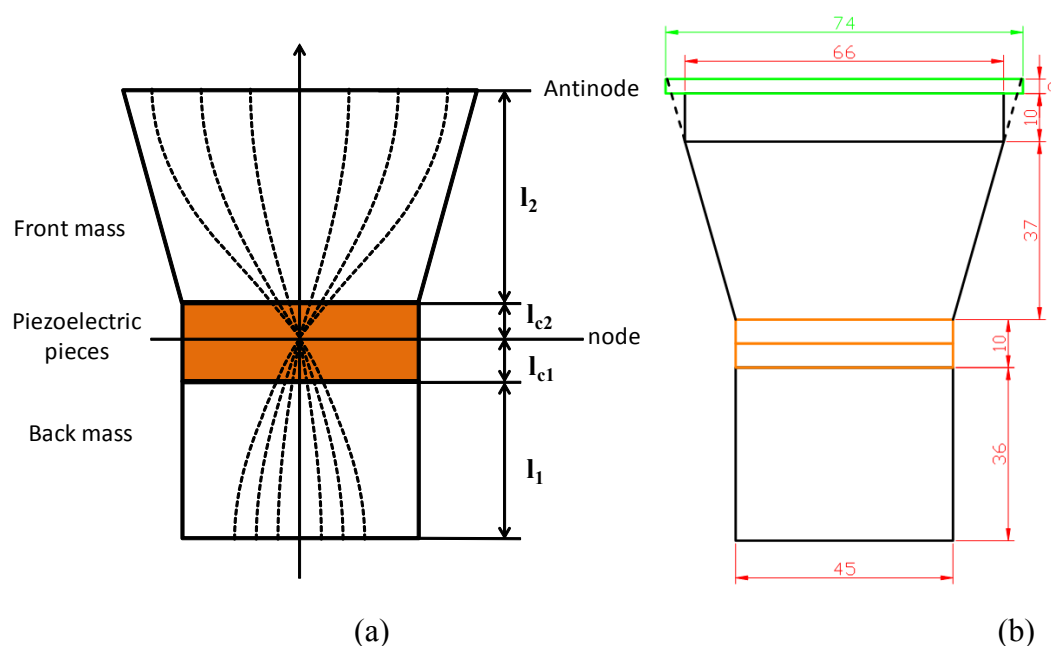


Fig. S1 (a) Diagram of the Langevin-type ultrasonic transducer. The dashed lines represent the half wavelength standing wave. (b) Size and structure of the ultrasonic microreactor's axial cross section. The dash line shows the approximated new circular truncated cone mass.

Table 1 The value of the parameters chose in the MATLAB procedure calculation

Parameter	$P / 10^3\text{ kg/m}^3$	$c / 10^3\text{ m/s}$
piezoelectric pieces	7.5	2.9
Back mass	7.9	5.8
Front mass	2.7	5.1

2. Experimental detail

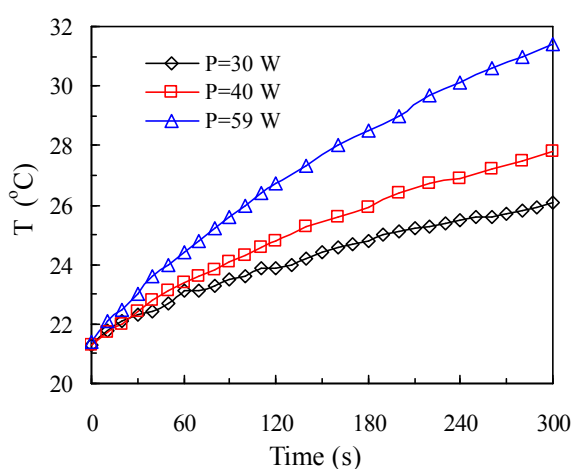
Gas flow was provided from a cylinder and controlled by a mass flow controller (D07-7B, Beijing Sevenstar Electronics, China, accuracy of 0.5% full scale). To stabilize the gas-liquid two phase flow, a large pressure barrier was added in the gas feeding line using a small-diameter fused silica capillary (inner diameter 50 μm ; length 30 mm). Deionized water was

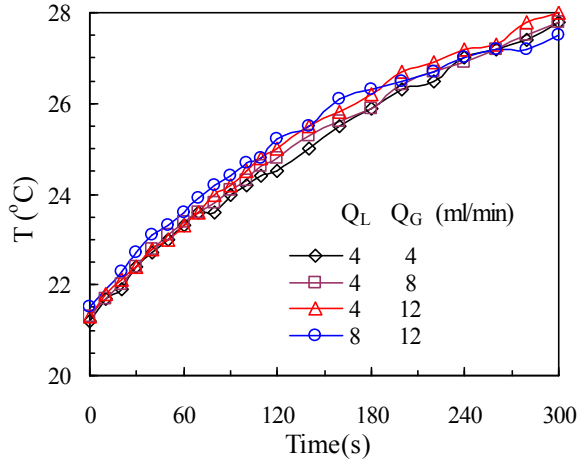
pumped by a high-precision digital piston pump (Beijing Satellite Manufacturing Factory). The temperature of the fluid was monitored by a K-type thermocouple (1 mm diameter) connected at the outlet of the microreactor.

The microchannel was fabricated in an Aluminum alloy plate using micromachining technology (FANUCKPC-30a) in our CNC Machining Center. The microreactor was connected with the feed and discharge pipes by a short stainless steel capillary (capillary with outer diameter 0.5 mm, inner diameter 0.2 mm at the inlet and outer diameter 1 mm, inner diameter 0.6 mm at the outlet). The capillary were directly inserted into the microchannel at the inlet and outlet and sealed by epoxy glue.

3. The temperature rise of the experiment system and its control

Temperature rise during the experiment with the fan running and fluids flowing was recorded. As shown in Fig. S2(a), the temperature increases with the prolong of experiment time and rise of ultrasound power. It's indicated that the higher is the input ultrasound power, the more is the energy absorbed by the fluid and then converted into heat. As shown in Fig. S2(b), the influence of flow rates on the temperature rise is not obvious in the measured time range. Generally, the lower is the flow rate, the longer is the residence time of fluid in the ultrasonic irradiated microreactor, which would leads to higher temperature rise. However, at lower flow rate, the time for heat exchange between the fluid and the air-cooled microreactor is also longer. That is to say, the heat dissipation time is longer at lower flow rate, which would offset the higher temperature rise caused by longer irradiation time. It can explain the less influence of flow rates on the temperature rise.





(a)

(b)

Fig.S2 (a) Temperature rise of the fluid at different ultrasound power. The flow rate of liquid and gas is $Q_L=4 \text{ ml/min}$, $Q_G=8 \text{ ml/min}$. (b) Temperature rise of the fluid at different flow rates. The power of the ultrasound is 40 W .

As shown in Fig. S2(a), at power of 40 W , the temperature increases about $6 \text{ }^\circ\text{C}$ in 5 minutes. It rises up to $10 \text{ }^\circ\text{C}$ at power of 59 W . This temperature rise is relatively high, especially when the system is used continuously. We think this problem can be solved if the air cooling system in our experiment is optimally designed. For example, a wind-guide-cover and one or two air fan with higher power can be used to enhance the heat dissipation capacity. Besides, if the electronic subsystem (especially the wave form of the ultrasonic generator) is further optimized, the energy efficiency of the system would be improved and less energy would be converted into heat, which could also reduce the temperature rise.

The gas-liquid mass transfer coefficient in our experimental system depends on the flow state of the gas-liquid two phase in the microchannel and the diffusion coefficient of CO_2 in water. With a temperature rise of $3 \text{ }^\circ\text{C}$, the change of the fluid property is very small, and so the change of flow state can be neglected. The diffusion coefficient of CO_2 in water rises about 7% when the temperature is increased by 3°C ³. Whether use the mass transfer coefficient defined by the penetration model

$$k_L = 2\sqrt{D_m / \pi\theta}$$

or the film model⁴

$$k_L = \frac{D_m}{\delta}$$

the rise of about 7% of the diffusion coefficient could lead to an increase of 7% of the mass

transfer coefficient at most. Compared with the high enhancement caused by ultrasound (between 330%-570%), we think the influence of temperature rise on mass transfer coefficient can be neglected in our experiment.

4. The influence of ultrasound on the gas-liquid flow

The gas-liquid slug flow in the microfluidic channel without and with the irradiation of ultrasound was shown in Fig. S3(a). When the ultrasound was exerted, all the gas bubbles in the microchannel oscillated vigorously (Fig. S3(b)). This fierce oscillation even leads to a fluctuation of the stable two-phase flow. As shown in Fig. S3(b), some bubbles moved close to each other and a few occasionally coalesced into a longer bubble.

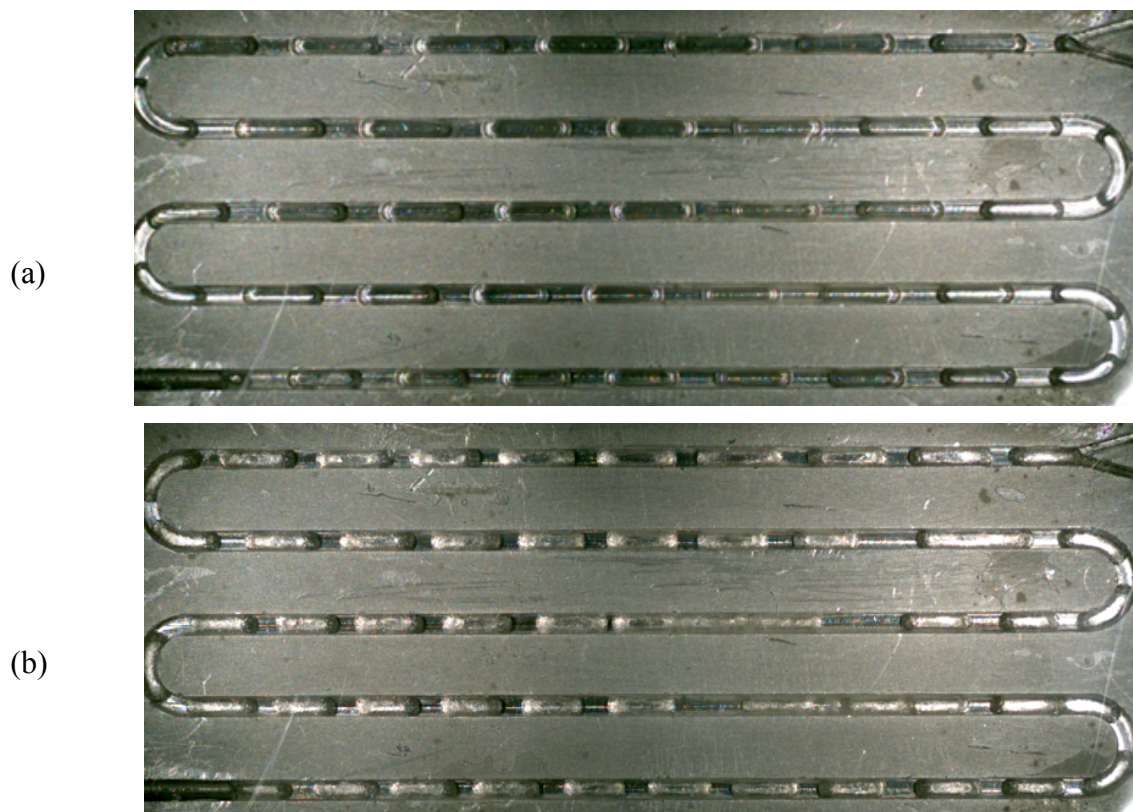


Fig. S3 The gas-liquid slug flow without (a) and with (b) the irradiation of ultrasound (70 W), $Q_L=4 \text{ ml/min}$, $Q_G=8 \text{ ml/min}$.

5. The output waveform of the ultrasonic generator

The output waveform of the ultrasonic generator was recorded with an oscilloscope by measuring the voltage supplied to the Langevin-type transducer. The wave form at power of 40 W was given in Fig. S4. The voltage signal has a period of about 13 ms, in which the voltage rises to a maximum and then drops.

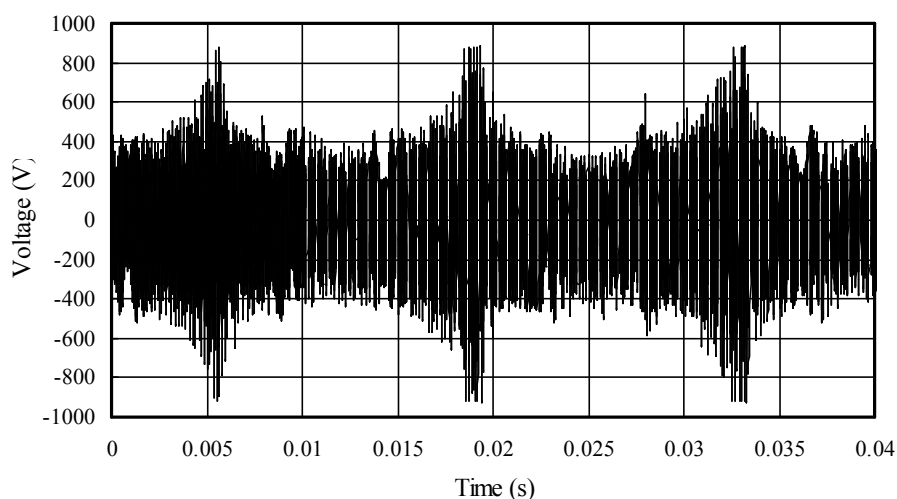


Fig. S4 The recorded voltage signal supplied to the transducer at power of 40 W .

6. Ultrasound power density

Ultrasound power density in the fluid is estimated by a calorimetric method^{5,6}. The temperature rise of the fluid was recorded by the thermocouple, when the air fan was turned out and the ultrasonic generator turned on (Fig. S5). The acoustic power density was determined from the temperature slope at the beginning of the ultrasound irradiation:

$$W = \rho c_p \left. \frac{\Delta T}{\Delta t} \right|_{t=0}$$

With ρ the density of the liquid and c_p its specific heat. At power of 40 W and 53 W , the power density was estimated to be 0.13 W/ml and 0.7 W/ml respectively. We didn't measure the temperature rise at power of 70 W , which is too fast to read by eyes and too high for the reactor to bear. But we can estimate its power density by the values at 40 W and 53 W , when assuming that the power density increases linearly with the total power input. The value estimated by this method is 1.4 W/ml .

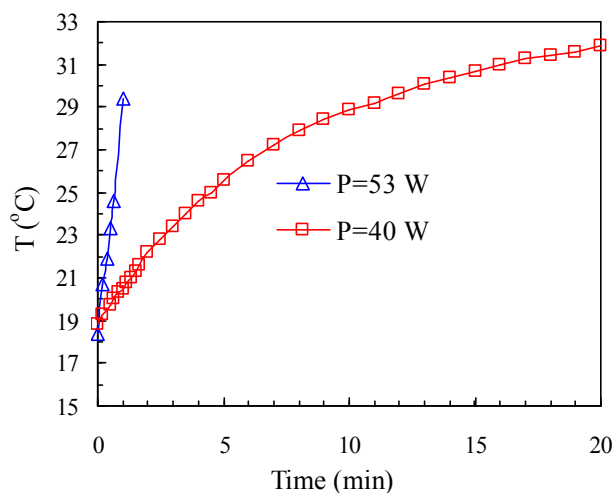


Fig. S5 Temperature rise of the fluid was recorded by the thermocouple connected at the outlet of the microreactor.

7. Video1 Captions

The detail of the slug bubble oscillation at power of 40 W was recorded by the high speed camera at frame rate of 100 000 fps. The actual total time of video1 is 23 ms , which is about 2 periods of the voltage signal. So the changing of the bubble surface vibration amplitude has two periods of rise and drop. The gas and liquid flow rate in the video: $Q_L=4$ ml/min , $Q_G=8$ ml/min .

References

1. S. Lin, The mechanism and design of ultrasound transducer, Science Press, 2004 (in chinese)
2. M. D. McCollum, B. F. Hamonic and O. B. Wilson, Transducers for Sonics and Ultrasonics, Technomic, Lancaster, PA, 1993
3. G. F. Versteeg, and W. P. M. van Swaaij, J. of Chem. and Eng. Data, 32, 29-34
4. M. N. Kashid, A. Renken and L. Kiwi-Minsker, Chem. Eng. Sci., 2011, 66, 3876-3897
5. J. M. Loning, C. Horst and U. Hoffmann, Ultrason.Sonochem.,2002, 9, 169-179
6. R.G. Macedo, B. Verhaagen, D. F. Rivas, J.G.E. Gardeniens, L.W.M. van der Sluis, P.R. Wesselink and M. Versluis, Ultrason. Sonochem., 2014, 21, 324-335